Monolithic Design and Fabrication of a 2-DOF Bio-Inspired Leg Transmission

Daniel M. Aukes, Onur Ozcan, and Robert J. Wood *

School of Engineering and Applied Sciences
Wyss Institute for Biologically Inspired Engineering
Harvard University, Cambridge MA.

Abstract. We present the design of a new two degree-of-freedom transmission intended for micro / meso-scale crawling robots which is compatible both with laminate manufacturing techniques and monolithic, "pop-up" assembly methods. This is enabled through a new design suite called "popupCAD", a computer-aided design tool which anticipates laminate manufacturing methods with a suite of operations which simplify the existing design workflow. The design has been prototyped at three times the anticpated scale to better understand the assembly and motion kinematics, and simulated to establish the basic relationships between the actuator and end-effector transmission ratios.

1 Introduction

The advent of new laminate-manufacturing techniques such as Printed-Circuit MEMS (PC-MEMS) [1, 2], Smart Composite Micro-structures (SCM) [3, 4], and Lamina Emergent Mechanisms (LEM) [5, 6] has enabled the development of a new class of millimeter-scale devices. These manufacturing techniques use a relatively small set of operations such as cutting, lamination, and folding to create a variety of mechanical components, such as hinges, structural elements, and springs. These devices are typically designed through the selective removal of material across neighboring material layers to create planar mechanisms. By using multiple materials in the laminate, the mechanical properties of these devices can be tuned for each component. Highly specialized devices can be developed through the iterative use of these operations, and discrete components can be added throughout the process. Using laser cutters to create precise alignment geometry, highly complex kinematics can also be created between hinged rigid bodies and utilized both for structures and mechanisms.

Through these new manufacturing techniques, a variety of new devices have been realized, from flying micro-robots inspired by bees [1] to crawling robots

* This material is based upon work supported by the National Science Foundation (grant numbers EFRI-1240383 and CCF-1138967) and the Wyss Institute for Biologically Inspired Engineering. Any opinions, findings, and conclusions or recommendations expressed in this material are those of the authors and do not necessarily reflect the views of the National Science Foundation.

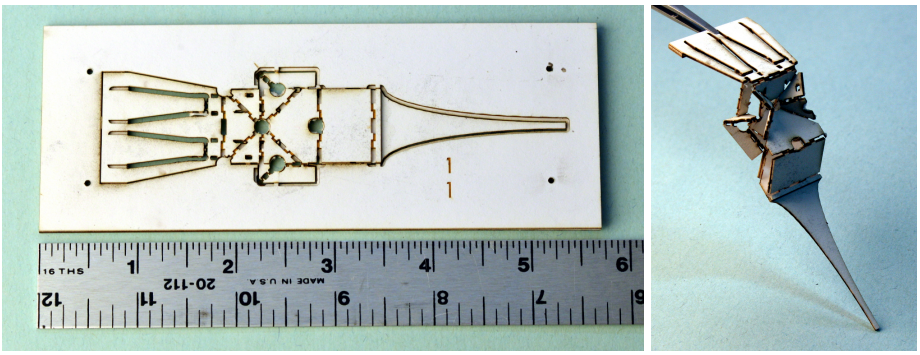

(a) (b)

Fig. 1: Prototype transmission in (a) flattened and (b) assembled configurations.

[7–9]. In addition, [2] demonstrates monolithic assembly techniques for faster, more precise manufacturing with a device called "Mobee". For all the potential of this concept, however, only this device has used monolithic "pop-up" fabrication techniques. This is due in part to the lack of design software which encapsulates laminate design and manufacturing rules; consequently the addition of assembly scaffolds adds too much complexity to the average design. To work around such complexities, designers split devices into simpler parts, ultimately relying on manual assembly and locking operations which require dexterity and expertise. Thus, manufacturing remains slow and error-prone.

In order to facilitate the transition from manual manufacturing of discrete components to more automated, monolithic fabrication of entire robots, we present preliminary work on a bio-inspired, two degree-of-freedom transmission to be used in the leg of a crawling robot, which is compatible with the concepts of PC-MEMS manufacturing and monolithic, "pop-up" assembly. This design is composed entirely of elements which begin flat and pre-assembled in a laminate, and by actuating and locking a single degree of freedom, are positioned into their assembled state.

2 Device Overview

The device shown in Figure 2a consists of many individual linkages connected through hinges on two sub-laminate layers. These linkages are arranged around four spherical linkages: two six-bar rotational linkages (6R) and two four-bar rotational linkages(4R). Both linkages start in their flattened state, but rotate in three-dimensional space about one point when actuated.

In combining the input and output stages of such linkages in various ways, interesting kinematic properties can be exploited. For example, the output stage of the 6R spherical linkage used in Figure 1 has the properties of a spherical joint, with three degrees of freedom in rotation. Two grounded spherical linkages

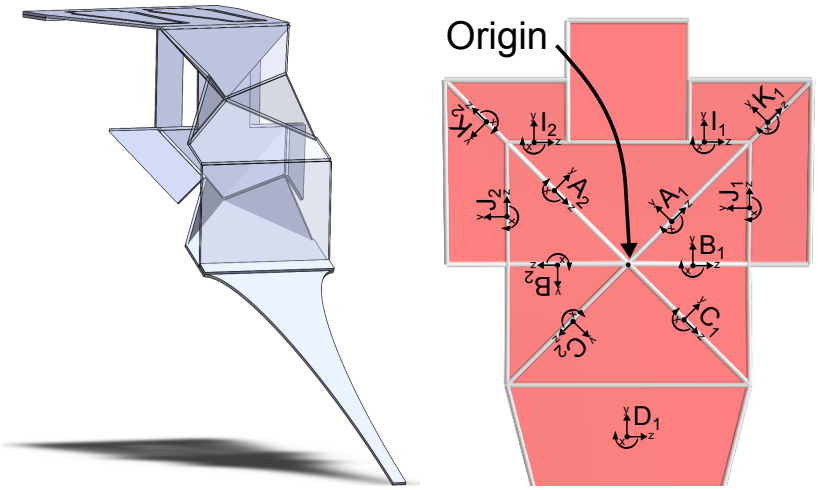

(a) (b)

Fig. 2: The full leg design is shown in in (a). Links of the upper 6R spherical mechanism are translucent . Reference frames for the three linkages on the bottom sublaminate are shown in (b).

whose output stages are rigidly connected, however, are more constrained in their motion, acting as a single degree-of-freedom rotational hinge. Similarly, four-bar linkages exhibit only a single degree of freedom between input and output stages, yet can impart highly nonlinear motion relationships between the two. Yet all these devices start flat and are thus compatible with PC-MEMS manufacturing processes, making them ideal building blocks for pop-up compatible designs.

In this design, the connection of these elementary building blocks mimics structures seen in biology. Multiple degrees of freedom can be seen in the human hip joint, for example, where ball-and-socket mechanisms in the bones and cartilege provide smooth rotation across a wide range of angles. Yet the motion of joints such as this is rarely constrained by a single mechanism but are complemented by a redundant set of muscles and tendons which route across and between joints, guiding, supporting and restricting motion. In this way, the leg mechanism, with its redundant-yet-constrained six bar linkgages, provides a much more limited range of motion than each subcomponent independently would capable of delivering – and in a way which is inherently more manufactuable. Parallels to this concept are prevalent in biological systems as well, where the capabilities of the integrated system are greater than the sum of its parts.

3 CAD Design, Fabrication, and Materials

The initial design of the device is carried out in Solidworks in order to test the design concept and perform initial kinematic simulations. However, the Solid-

works design only includes basic sketches of the layers, and not detailed drawings of features. The actual design used for fabrication is done using a new Computer Aided Design and Manufacturing (CAD/CAM) application called popupCAD [10]. Traditional CAD/CAM software, such as Solidworks, does not have any built-in tools to help with unconventional manufacturing methods such as PC-MEMS or SCM. On the other hand, popupCAD is specifically designed for layer-based manufacturing methods. The software automatically generates cut files using PC-MEMS and Pop-Up MEMS design and fabrication rules. It also has several operations specific to layer-based design and fabrication methods (e.g. generating support structures around features). In order to take advantage of these software features, we have imported the Solidworks sketches into popupCAD as guidelines, completed the design by adding the necessary PC-MEMS features such as hinges and support web, and generated the cut files in popupCAD. An example initial cut file and the final cut file used to fabricate the device is shown in Figure 3.

(a) First Pass Cuts (b) Second Pass Cuts

Fig. 3: First and Second Pass Cuts

The device is fabricated using SCM method and Pop-Up Manufacturing / Assembly. Due to the kinematic loops, the device cannot fit on a single linkage sublaminate. Therefore the complete device requires two linkage sublaminates. Each linkage sublaminate consists of five layers: two outer cardboard layers for rigid links, a polyimide (Kapton) layer that forms the joints and two adhesive (double sided acrylic tape) layers that bond these functional layers. In order to generate the two linkage sublaminates needed for the device, we need 11 layers: five layers per linkage sublaminate and a layer of adhesive that connects the two linkage sublaminates. The linkage sublaminate layers are first bulk micromachined individually using a CO2 laser (Universal Laser Systems, PL3.50) and a layup is formed using pin alignment. During fabrication, the rigid links are where all the materials are present and hinges are where the cardboard is cut out. The cut files for these first cuts are automatically generated by popupCAD on the locations that cannot be accessed during the release cut because there is material at the same location on different layers. The only exception to this process is the middle layer, the adhesive connecting two linkage sublaminates. This layer cannot be supported from outside like the other adhesive layers, because such support would result with two linkage sublaminates bonding to each other at

undesired locations. Instead, this layer includes adhesive islands that should be placed carefully. In order to solve this issue, we cut a negative of this island template from the polyimide film and used it as a mask to selectively deposit a spray adhesive (3M Hi-Strength 90 Spray Adhesive.)

4 Kinematics

Frame	A_1	B_1	C_1	D_1	A_2	B_2	C_2	D_2	E_1	F_1	G_1	H_1	E_2	F_2	G_2	H_2	I_1	J_1	K_1	L_1	I_2	J_2	K_2	L_2
Parent	Base	A_1	B_1	C_1	Base	A_2	B_2	C_2	Base	E_1	F_1	G_1	Base	E_2	F_2	G_2	Base	A_1	I_1	K_1	Base	A_2	I_2	K_2
a	0	0	0	0	0	0	0	0	1	0	0	0	1	0	0	0	1	0	0	0	1	0	0	0
a_i	0	0	0	0	0	0	0	0	0	0	0	0	0	0	0	0	0	0	0	0	0	0	0	0
α_i	t	t	t	t	t	t	t	t	t	t	t	t	t	t	t	t	0	t	$\pi/4$	$\pi/4$	0	t	$\pi/4$	$\pi/4$
θ_i	q^*_{c1}	q^*_{b1}	q^*_{c1}	0	q^*_{a2}	q^*_{b2}	q^*_{c2}	0	q^*_{e1}	q^*_{f1}	q^*_{g1}	0	q^*_{e2}	q^*_{f2}	q^*_{g2}	0	q^*_{i1}	q^*_{j1}	q^*_{k1}	0	q^*_{i2}	q^*_{j2}	q^*_{k2}	0

* indicates state variable. In this design, $t = \pi/4$

Table 1: Denavit-Hartenberg Parameters. The variable t indicates a design parameter which can be modified to alter the transmission ratio.

Four kinematic loops determine the transmission characteristics between the actuators and the leg. The two 6R spherical linkages establish one kinematic loop each, and the two 4R spherical linkages define two additional kinematic loops. One of the six-bar linkages is shown in Figure 2b. Frames A_1,B_1,C_1,D_1,A_2,B_2,C_2, and D_2 belonging to this linkage can be used to generate the kinematic loop equations, which are generated by aligning the basis vectors of frames D_1 and D_2 using the equations

$$0 = \widehat{x}_1 \cdot \widehat{x}_2 - 1 \tag{1}$$

$$0 = \widehat{y}_1 \cdot \widehat{y}_2 - 1 \tag{2}$$

$$0 = \widehat{z}_1 \cdot \widehat{z}_2 - 1, \tag{3}$$

where x_1, y_1, z_1 and x_2, y_2, z_2 represent the orthonormal basis vectors for frames D_1 and D_2, respectively. These three equations establish a relationship between the six state variables $q_{a1}, q_{b1}, q_{c1}, q_{a2}, q_{b2}$, and q_{c2}, establishing that the output frame D_1 has three rotational degrees of freedom. Between the newtonian reference frame(the base frame) and D_1, this mechanism can be treated as a spherical joint.

The second 6R spherical linkage consisting of frames E_1,F_1,G_1,H_1,E_2,F_2,G_2, and H_2 behaves as the first, establishing the spherical loop constraint equations between H_1 and H_2 using Equations (1-3). The outputs of the two 6R spherical linkages are connected by a 2R linkage which enforces orientation between the frames D_1 and H_1 using Equations (1-3) and

$$0 = (\widehat{n}_y \times \widehat{d}_{1z}) \cdot (\widehat{n}_y \times \widehat{d}_{1z}) - 1, \tag{4}$$

where n_z represents the z-oriented basis vector of the Newtonian reference frame.

The two 4R spherical linkages, defined by the frames $\{A_1, I_1, J_1, K_1\}$ and $\{A_2, I_2, J_2, K_2\}$ respectively, are used to transmit the linear forces from each piezo-electric actuator into frames A_1 and A_2 of the bottom 6R spherical linkage. Frames J_1 and J_2 are aligned with K_1 and K_2 respectively using Equations (1-3). Thus for the four kinematic loops, 10 constraint equations can be established for the 12 state variables, establishing a two degree-of-freedom system.

Using the principle of virtual work, two Jacobians of the constraint equations may be obtained for the independent and dependent state variables by taking the partial derivative of the vector of constraint equations $\mathbf{f}(q)$ with respect to to each variable in $\mathbf{q}_{ind}$ and $\mathbf{q}_{dep}$ to obtain $\mathbf{J}_{ind}$ and $\mathbf{J}_{dep}$, respectively. Two state variables must be selected for the independent state vector, so in this case we pick $\mathbf{q}_{ind} = [q_{i1}, q_{i2}]^T$. The rest are put in $\mathbf{q}_{dep}$. The Jacobians can then be derived according to

$$0 = J_{ind}\dot{\mathbf{q}}_{ind} + J_{dep}\dot{\mathbf{q}}_{dep}, \tag{5}$$

$$-J_{dep}\dot{\mathbf{q}}_{dep} = J_{ind}\dot{\mathbf{q}}_{ind}, \text{ and} \tag{6}$$

$$\dot{\mathbf{q}}_{dep} = \underbrace{-J_{dep}^{-1}J_{ind}}_{T}\,\dot{\mathbf{q}}_{ind}. \tag{7}$$

The position of the actuator input and leg output can be represented in terms of the independent and dependent state variables $\mathbf{q}_ind$ and $\mathbf{q}_dep$, independently. This permits the calculation of input and output Jacobians as

$$\dot{\mathbf{q}}_{in} = A\dot{\mathbf{q}}_{ind} + B\dot{\mathbf{q}}_{dep} \tag{8}$$

$$\dot{\mathbf{q}}_{out} = C\dot{\mathbf{q}}_{ind} + D\dot{\mathbf{q}}_{dep}. \tag{9}$$

By combining Equations (7-9), a direct relationship between input and output velocities can be determined, as

$$\dot{\mathbf{q}}_{in} = \underbrace{(A + BT)}_{E}\,\dot{\mathbf{q}}_{ind} \tag{10}$$

$$\dot{\mathbf{q}}_{out} = \underbrace{(C + DT)}_{F}\,\dot{\mathbf{q}}_{ind} \tag{11}$$

$$\dot{\mathbf{q}}_{out} = FE^{-1}\dot{\mathbf{q}}_{in}. \tag{12}$$

These equations permit the calculation of the input/output transmission ratios and the resulting output path as a function of a valid initial state, as shown in Figure 4.

5 Discussion

A motion study has been performed for the constrained mechanism, determining output trajectories and velocities as a function of actuator input signal. A variety of input signals were tested, with the results from two simulations shown in

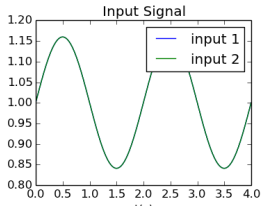

(a) Input Plot 1

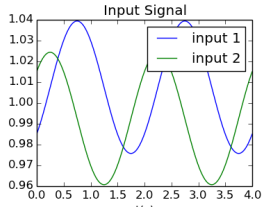

(b) Input Plot 2

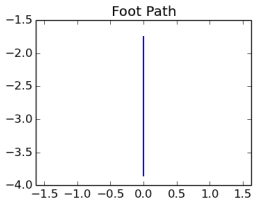

(c) Z-Y Output Plot 1

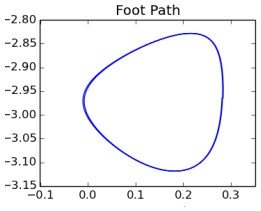

(d) Z-Y Output Plot 2

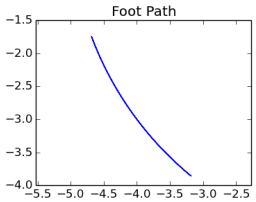

(e) X-Y Output Plot 1

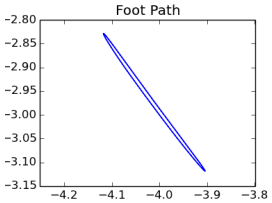

(f) X-Y Output Plot 2

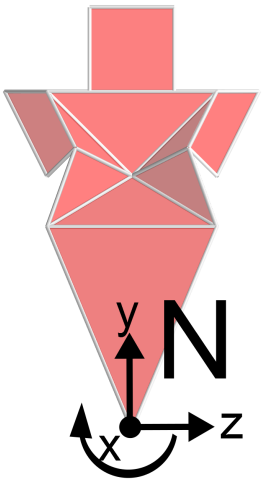

(g) Output Reference Frame

Fig. 4: Transmission Plots for two different input signals. In the first simulation, inputs are driven in phase with sinusoidal amplitudes of 0.5. In the second simulation, a phase shift of $\pi/2$, input offset of .06, and amplitude of .1 is used to achieve a more-circular path.

Figure 4. As can be seen in the plots of the two simulations, driving the signals in phase with each other produces lift motion in the leg (along $\widehat{n}_y$), and differential signals produce swing motion (motion along $\widehat{n}_z$). By supplying combinations of input and phase offset, a variety of trajectories can be produced, as seen in the second simulation of Figure 4.

6 Conclusions and Future Work

In this paper we have presented the initial design and kinematic evaluation for a bio-inspired leg transmission, suitable for integration into new crawling robot designs. Work is continuing in this direction, both on leg design and integration issues. While this transmission offers similar capabilities to the legs employed in current-generation legs, it offers the additional compatibility with monolithic

assembly methods which can help reduce errors during assembly and speed up the process. As design criteria for these new robots become more developed, the models developed here can become the basis for further design and optimization of the transmission. In particular, the study of the dynamics of this new device will be crucial in evaluating and comparing current and future designs. In addition, by deriving the inverse kinematics of the leg, complex custom foot trajectories may be generated as a function of the two actuators.

References

1. J. P. Whitney, P. S. Sreetharan, K. Y. Ma, and R. J. Wood, "Pop-up book MEMS," *Journal of Micromechanics and Microengineering*, vol. 21, no. 11, p. 115021, Nov. 2011. [Online]. Available: http://stacks.iop.org/0960-1317/21/i=11/a=115021?key=crossref.4ebe6c2c4c4804ab44e0dfb88e1b355e
2. P. S. Sreetharan, J. P. Whitney, M. D. Strauss, and R. J. Wood, "Monolithic fabrication of millimeter-scale machines," *Journal of Micromechanics and Microengineering*, vol. 22, no. 5, p. 055027, May 2012. [Online]. Available: http://stacks.iop.org/0960-1317/22/i=5/a=055027?key=crossref.491915c123069b686e444a77780882a9
3. R. J. Wood, S. Avadhanula, R. Sahai, E. Steltz, and R. S. Fearing, "Microrobot Design Using Fiber Reinforced Composites," *Journal of Mechanical Design*, vol. 130, no. 5, p. 052304, 2008. [Online]. Available: http://link.aip.org/link/?JMDEDB/130/052304/1http://mechanicaldesign.asmedigitalcollection.asme.org/article.aspx?articleid=1449731
4. A. M. Hoover and R. S. Fearing, "Fast scale prototyping for folded millirobots," *2008 IEEE International Conference on Robotics and Automation*, pp. 1777–1778, May 2008. [Online]. Available: http://ieeexplore.ieee.org/lpdocs/epic03/wrapper.htm?arnumber=4543462
5. J. O. Jacobsen, B. G. Winder, L. L. Howell, and S. P. Magleby, "Lamina Emergent Mechanisms and Their Basic Elements," *Journal of Mechanisms and Robotics*, vol. 2, no. 1, p. 011003, 2010. [Online]. Available: http://mechanismsrobotics.asmedigitalcollection.asme.org/article.aspx?articleid=1484914
6. P. S. Gollnick, S. P. Magleby, and L. L. Howell, "An Introduction to Multilayer Lamina Emergent Mechanisms," *Journal of Mechanical Design*, vol. 133, no. 8, p. 081006, 2011. [Online]. Available: http://mechanicaldesign.asmedigitalcollection.asme.org/article.aspx?articleid=1450638
7. A. Baisch and C. Heimlich, "HAMR3: An autonomous 1.7 g ambulatory robot," *Intelligent Robots and ...*, pp. 5073–5079, 2011. [Online]. Available: http://ieeexplore.ieee.org/xpls/abs_all.jsp?arnumber=6095063
8. A. Baisch, O. Ozcan, B. Goldberg, D. Ithier, and R. Wood, "High Speed Locomotion for a Quadrupedal Microrobot," *International Journal of Robotics Research(to appear)*, 2014.
9. A. Hoover, E. Steltz, and R. Fearing, "RoACH: An autonomous 2.4g crawling hexapod robot," in *2008 IEEE/RSJ International Conference on Intelligent Robots and Systems*. IEEE, Sep. 2008, pp. 26–33. [Online]. Available: http://ieeexplore.ieee.org/lpdocs/epic03/wrapper.htm?arnumber=4651149
10. D. M. Aukes, B. Goldberg, M. R. Cutkosky, and R. J. Wood, "An Analytic Framework for Developing Inherently-Manufacturable Pop-up Laminate Devices," *Smart Materials and Structures (submitted for review)*, 2014.